



RESEARCH ARTICLE

Amyloidogenicity assessment of transthyretin gene variants

Nicolai B. Grether¹, Felix Napravnik¹, Thomas Imhof², Reinhold P. Linke³, Jan H. Bräsen⁴, Jessica Schmitz⁴, Maïke Dohrn^{5,6}, Christian Schneider¹, Martin K. R. Svačina¹, Jörg Stetefeld⁷, Manuel Koch^{2,8,*}  & Helmar C. Lehmann^{1,*} 

¹Department of Neurology, Faculty of Medicine and University Hospital of Cologne, University of Cologne, Cologne, Germany

²Institute for Dental Research and Oral Musculoskeletal Biology and Center for Biochemistry, University of Cologne, Cologne, Germany

³Reference Center of Amyloid Diseases, Munich, Germany

⁴Nephropathology Unit, Institute of Pathology, Hannover Medical School, Hannover, Germany

⁵Department of Neurology, Medical Faculty of the RWTH Aachen University Aachen, Germany

⁶Dr. John T. Macdonald Foundation, Department of Human Genetics and John P. Hussman Institute for Human Genomics, University of Miami, Miller School of Medicine, Miami, Florida, USA

⁷Department of Chemistry, University of Manitoba, Winnipeg, Canada

⁸Center for Molecular Medicine Cologne (CMMC), University of Cologne, Cologne, Germany

Correspondence

Helmar C. Lehmann, Department of Neurology, Medical Faculty, University Hospital of Cologne, Kerpener Str. 62, D-50937 Cologne, Germany. Tel: +49 221 478 87091; Fax: 0221 478 87309; E-mail: helmar.lehmann@googlemail.com

Funding Information

The study was funded by the German Research Foundation: FOR2722 to M. Koch.

Received: 23 June 2022; Accepted: 24 June 2022

Annals of Clinical and Translational Neurology 2022; 9(8): 1252–1263

doi: 10.1002/acn3.51626

*Joint senior authorship.

Abstract

Objective: Hereditary transthyretin-mediated amyloidosis is a treatable condition caused by amyloidogenic variants in the *transthyretin*-gene resulting in severe peripheral neuropathy or cardiomyopathy. Only about a third of over 130 known variants are clearly pathogenic, most are classified as variants of uncertain significance. A clear delineation of these into pathogenic or non-pathogenic is highly desirable but hampered by low frequency and penetrance. We thus sought to characterize their amylogenic potential by an unbiased in vitro approach. **Methods:** Thioflavin T and turbidity assays were used to compare the potential of mammalian cell expressed wt-transthyretin and 12 variant proteins (either variants of uncertain significance, benign, pathogenic) to aggregate and produce amyloid fibrils in vitro. As proof of principle, the assays were applied to transthyretin-Ala65Val, a variant that was newly detected in a family with peripheral neuropathy and amyloid deposits in biopsies. In silico analysis was performed to compare the position of the benign and pathogenic variants. **Results:** Transthyretin-Ala65Val showed a significantly higher amyloidogenic potential than wt-transthyretin, in both turbidity- and Thioflavin T-assays, comparable to known pathogenic variants. The other eight tested variants did not show an increased amyloidogenic potential. In silico structural analysis further confirmed differences between pathogenic and benign variants in position and interactions. **Interpretation:** We propose a biochemical approach to assess amyloidogenic potential of transthyretin variants. As exemplified by transthyretin-Ala65Val, data of three assays together with histopathology clearly demonstrates its amyloidogenicity.

Introduction

Amyloidogenic transthyretin (TTR) amyloidosis (ATTR) is a severe systemic disease caused by either wild-type transthyretin (ATTR_{wt} amyloidosis) or by pathologic mutations in the *TTR* gene (ATTR_v amyloidosis). While ATTR_{wt} amyloidosis occurs in high age, is slowly

progressive, and rarely affects the peripheral nerves, ATTR_v amyloidosis is a rapid-progressive disease that leads to polyneuropathy, cardiomyopathy, and autonomic or renal dysfunction. If untreated, it leads to disability and death typically within 10 years after diagnosis.^{1,2} There are over 130 known mutations in the *TTR* gene so far. Some of them are clearly pathogenic, such as

TTR-Val142Ile, resulting in familial amyloid cardiomyopathy, or TTR-Val50Met, which typically leads to familial amyloid polyneuropathy.^{3,4} Others are considered non-pathogenic. The majority are deemed either (i) variants of uncertain significance (VUS) or (ii) mutations with conflicting interpretations of pathogenicity,⁵ (Fig. 1). Furthermore, compound heterozygotic carriers have been described and the relevance of benign variants that protect from amyloidosis even in the presence of a known pathogenic variant is largely unknown. Many variants have only been described in one individual or family. Despite being an autosomal dominantly inherited disorder, penetrance can be low, depending on the variant.⁶ Additionally, despite being a systemic amyloid disease,⁷ it can be difficult to detect amyloid fibrils in tissue samples, e.g. after nerve biopsy. These shortcomings, in addition to the general low frequency of the disease, prevents an unequivocal classification of pathogenic and non-pathogenic mutations.

Since an early diagnosis and treatment is fundamental to decelerate or suspend ATTR_v amyloidosis, it is important to know the pathogenicity of TTR variants. In this

study we explored in vitro whether there is evidence that TTR-variants have an increased potential to form amyloid fibrils or protein aggregation in comparison to wt-TTR. As proof of principle, these in vitro tests were applied to TTR-Ala65Val, a variant that was observed in a family with peripheral neuropathy. We further anticipated that due to the large number and low penetrance of pathogenic TTR, single case reports of asymptomatic patients can be potentially misleading.⁸⁻¹⁰ Thus, VUS of TTR that were reported in single patients or in one family were selected and assessed additionally.

Material and Methods

Literature analysis of TTR variants

Literature was searched for known amyloidogenic variants, and variants that have been suggested to be apathogenic, but where clinical data were sparse, using NCBI PubMed, NCBI ClinVar and Google Scholar database. Most of the variants we selected were only described in

Distribution of clinical significance of described TTR variants (n=140)

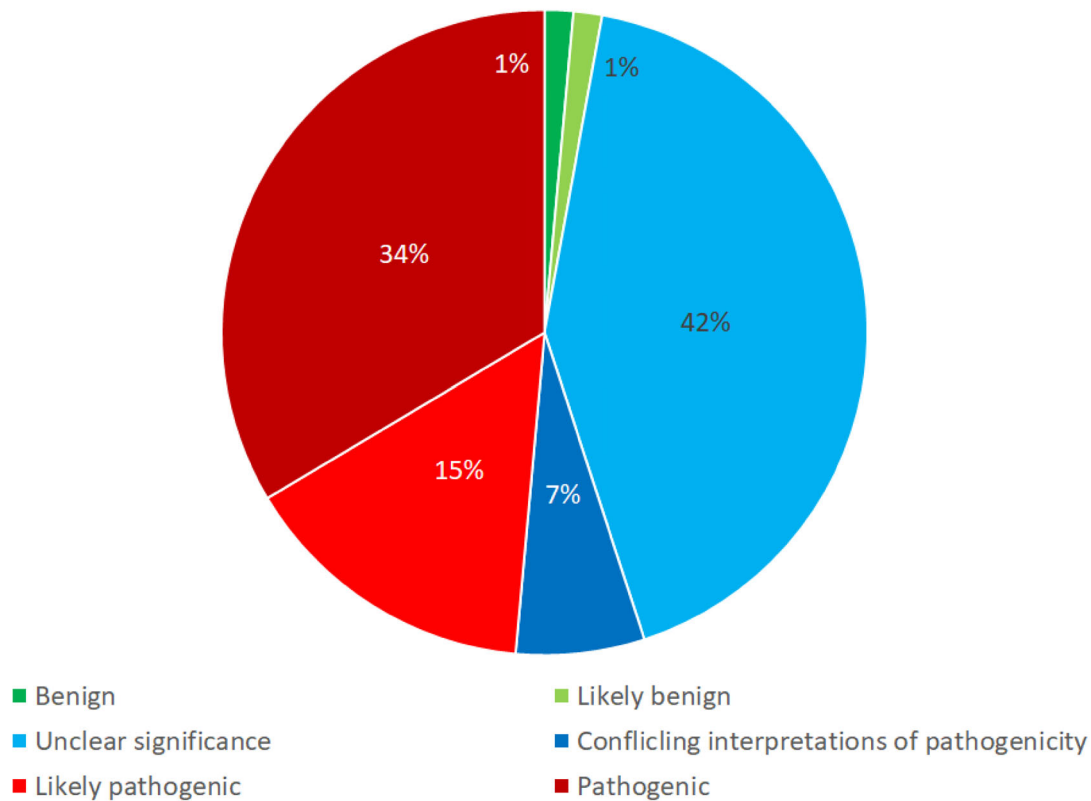


Figure 1. Distribution of clinical significance of TTR variants causing protein changes according to ClinVar (<https://www.ncbi.nlm.nih.gov/clinvar>, 28.03.2021 12:56). 1% were considered to be benign and likely benign respectively. 42% were classified as VUS, 7% as conflicting interpretations of pathogenicity, 15% as likely pathogenic and 34% as pathogenic.

one patient or one family. The assessed variants are listed in Table 1.

Cloning and protein purification

Depending on the localization of the target mutation, mutations were introduced by point-mutated primers or site-directed overlap extension PCR. Afterwards, TTR and TTR-variants were cloned into sleeping beauty vectors modified with an N- or C-terminal Twin Strep-tag and the sequences were verified by Sanger sequencing (Microsynth Seqlab, Göttingen, Germany).

Near confluent HEK293-EBNA cells were transfected using FuGENE HD reagent (Promega, Madison, WI) and selected by 3 µg/mL puromycin in DMEM/F12 medium containing 7% fetal calf serum (FCS) (Gibco, ThermoFisher Scientific, Waltham, MA) for 5 days. The selected cells were then transferred into Nunc™ TripleFlask™ (ThermoFisher Scientific), expanded for 1 week and then protein expression was induced with 1 µg/mL doxycycline in 2% FCS/DMEM/F12 medium. Every third day, supernatants were collected and replaced with 135 mL fresh doxycycline containing DMEM/F12 medium. For the Strep affinity purification the medium was adjusted to pH 8, filtered and then purified via Strep-Tactin XT™ sepharose columns (IBA GmbH, Göttingen, Germany) according to the manufacturer protocol. To determine the protein concentration, the absorbance at OD280 was measured with a BioPhotometer (Eppendorf, Hamburg, Germany).

Dialysis of buffers and final concentration

For ThT-binding and turbidity measurement, specimens were dialyzed in 200 mmol/L acetate buffer containing 100 mmol/L NaCl and 1 mmol/L EDTA at pH 5.0 with Slide-A-Lyzer MINI Dialysis Units (ThermoFisher Scientific). Afterwards, specimens from multiple columns were

pooled and concentration was measured with a BioPhotometer (Eppendorf, Hamburg, Germany). Proteins were diluted with respective buffer to a final concentration of 0.244 mg/mL.

For time course turbidity assay, proteins were dialyzed against phosphate buffer solution (20 mmol/L sodium phosphate, 100 mmol/L NaCl, 1 mmol/L EDTA, pH 7.6) using a dialysis tube (VISKING, SERVA, Heidelberg, Germany) with a volume per length of 2 mL/cm and a molecular weight cut-off of 12–14 kDa. After dialysis, the OD280 of each TTR-variant was measured with a BioPhotometer (Eppendorf, Hamburg, Germany) and the gained protein concentrations were equaled by adding buffer (20 mmol/L sodium phosphate, 100 mmol/L NaCl, 1 mmol/L EDTA, pH 7.6), down to a protein concentration of 0.6 mg/mL.

Turbidity measurement

To estimate the amount of aggregated protein in the solutions, turbidity assays with an UV/VIS spectrophotometer (Multiskan GO, ThermoFisher Scientific) were performed. All the specimens were incubated at 37°C for 72 h. We vortexed each specimen for 5 s directly before transferring them into a transparent F-bottom 96-well plate (Greiner Bio-One, Germany). The experiment was done with 300 µL protein solution per well at a wavelength of 400 nm. The mean value was created by 10 single measurements. To calculate the final turbidity values of the protein solutions, the corresponding solution buffers (blanks) values were subtracted from the measured protein solutions values. Each specimen was at least measured four times in duplicate and showed similar results.

In vitro aggregation time course

This assay was performed to observe the time course of aggregation of the different TTR-variants over 25 h. A microplate reader (Infinite M1000, Tecan Trading AG) was used to monitor the formation of amyloid in the specimens.

Transparent 96-well plates (Nunc MaxiSorp™, flat bottom, ThermoFisher Scientific) were used for the measurements. The aggregation of the protein solutions was induced by adding 80 µL acetate buffer (400 mmol/L sodium acetate, 100 mmol/L KCl, 1 mmol/L EDTA, pH 4.0) and 20 µL phosphate buffer (20 mmol/L sodium phosphate, 100 mmol/L NaCl, 1 mmol/L EDTA, pH 7.6) to 100 µL of protein solution ($c = 0.6$ mg/mL) per well, which led to a pH of 5.0 in these solutions. To the protein solution wells without induction of aggregation 100 µL of the phosphate buffer were added, so the concentration and volume per well were equal to the ones with induction at 200 µL and 0.3 mg/mL. All the other

Table 1. Overview of cloned TTR-variants (ClinVar-analysis, accessed 28.03.2021, 12:21).

TTR-variants	Clinical significance	References
Gly26Ser	Benign	11
Thr139Met	Conflicting interpretations of pathogenicity	12,13
Arg124Cys	Uncertain significance	14
Pro122Arg	Not listed	15
Gly121Ser	Uncertain significance	16
Ala129Val	Uncertain significance	17
Arg124His	Conflicting interpretations of pathogenicity	18
Ala129Thr	Uncertain significance	13
Val50Met	Pathogenic	4
Val142Ile	Pathogenic	3
Phe53Leu	Pathogenic	19
Ala65Val	Uncertain	

wells without protein solution were filled with 200 μ L phosphate buffer, to avoid measurement errors.

Measurements with the microplate reader were performed at a wavelength of 400 nm and a temperature between 36.5 and 37.5°C for 24 h, in an interval of 7 min between measurements. No shaking was applied. Each measurement was repeated with different protein aliquots and showed similar results.

Thioflavin T binding

As another method to test amyloidogenic potential of TTR variants, Thioflavin T (ThT)-staining was performed. ThT is a reagent that intercalates into amyloid fibrils and then induces a new emission spectrum.²⁰ ThT-staining of TTR-Ala65Val and VUS have been done independently on different days using fresh buffers and ThT respectively, which explain differences in emission signal between the two ThT-assays. Fluorescence emission is an arbitrary unit (AU), values can only be compared to ones of the same run.

We first prepared a stock solution with 10 mL PBS and 80 mg ThT (Sigma Aldrich, St. Louis, MO). We mixed 1 mL of the stock solution with 9 mL PBS to get a working solution. For the final solution, 1 mL of the working solution was diluted in 50 mL PBS. 150 μ L of the final solution were given into a flat bottom black Nunclon™ Sphera™ 96-wellplate (ThermoFisher Scientific) with 50 μ L of the respective protein solution that had been incubated at 37°C for 7 days. Plates were incubated at 37°C for 15 min. Light emission was measured using a Tecan i-control plate reader (Tecan Trading AG). Specimens were excited with 450 nm wavelength, emission was measured at 482 nm. Gain was set to 110, number of flashes to 20, flash frequency to 400 Hz, 1000 μ sec integration time, 10 msec settle time and z-position of 20 000 μ m at 37°C. Each mean value was the average of 26 single measurements. We used the respective buffer as a blank control. Background radiation from blank control was subtracted from the values. Measurements have been repeated twice with different aliquots of the proteins and showed similar results.

Congo red staining on patient samples

In order to detect amyloid deposits, congo red staining has been performed on adipose tissue of P2. Therefore, an established standard protocol was used.²¹

Congo red and TTR staining on patient samples

The adipose tissue aspirate was pressed overnight (10 kg), fixed in 4% neutral buffered formaldehyde and stained

for congo red as described.²¹ The cover slips were removed without manipulation by incubation in xylene-acetone until the coverslips fell off spontaneously. Afterwards, the samples were pretreated with pepsin solution (1 h, 37 °C, Zytomed Systems, Berlin, Germany) and afterwards immunostained with polyclonal rabbit anti-ATTR (clone TIE, amYmed, Munich, Germany) at a dilution of 1:10 for 120 min using an automated platform (Ventana ULTRA; Ventana Medical Systems, Tucson, AZ 85755) with DAB chromogen.

Statistics

For statistical analysis, GraphPad Prism (GraphPad software, San Diego, CA) and One-way multiple comparison ANOVA-test were used. *p*-values below 0.05 were considered statistically significant.

Results

Description of the family

A 60-year-old male patient presented with paresthesia and pallesthesia of the lower limbs, as well as reduced muscle tendon reflexes. Nerve conduction studies detected a slight sensory, predominantly axonal peripheral neuropathy with only slight reduction of sensory NCV in the sural nerve (Table 2). Sympathetic skin response revealed autonomic nervous system dysfunction. Echocardiography showed a left ventricular hypertrophy. No renal impairments were described. For further references, this index patient will be called “Patient 1” or “P1”.

At the age of 71 years, P1’s father was diagnosed with severe peripheral neuropathy. He will be further referenced as “P2”. Symptoms started at the age of 69 years with a progressive weakness of both lower limbs. In the course of the disease, he could not sit up without help anymore, and developed weakness of the upper limbs. He also described prickling, *pins and needles* and neuropathic pain in both arms and feet, as well as a decreasing ability to perceive temperature. Furthermore, he described

Table 2. Nerve conduction studies of the patients.

Nerve	NCS of P1 (year 2012)	NCS of P2 (year 2020)
Motor nerves (CMAP, conduction velocity)		
Tibial nerve (right)	1.9 mV, 43 m/s	13.3 mV, 40 m/s
Median nerve (right)	4.2 mV, 47 m/s	–
Sensory nerves (SNAP, conduction velocity)		
Sural nerve (right)	5 μ V, 38 m/s	5 μ V, 38 m/s
Median nerve (right)	2.9 μ V, 49 m/s	13 μ V, 50 m/s
Ulnar nerve (right)	2.2 μ V, 54 m/s	–

orthostatic dysregulation, erectile dysfunction, as well as problems with defecation with alternating diarrhea and obstipation. He lost around 18 kg of body weight unintentionally over the course of 3 years. The clinical examination showed a cachectic patient with paresis of dorsiflexors and knee-extensors, generalized reduction of muscle strength and weak or extinct tendon reflexes. He furthermore showed distal paresthesia and generalized muscle atrophy. Nerve conduct studies revealed a sensory and motor axonal neuropathy (Table 2). No renal or cardiac impairments were described in P2.

P2's father had died at the age of 75, also showing unintentional weight loss, progressive disability to walk and weakness of the limbs. He will further be called "P3". No nerve conduct studies or genetic testing had been performed on P3.

Genetic analysis in both P1 and P2 showed the heterozygous TTR variant TTR-Ala65Val (c.194C > T), which to our knowledge had not been described before.

Turbidity measurement and time course of wt-TTR, pathogenic variants and TTR-Ala65Val

In this first assay, the variant's tendency to aggregate was assessed. Amyloid fibrils are aggregates of misfolded TTR monomers, also called *pre-amyloid*. Thus, the detection of an increased amount of protein aggregation is a sign of increased formation of amyloid fibrils. Turbidity measurement is an established assay for protein aggregation.²²

TTR-Ala65Val (0.245, SD 0.006) as well as known pathogenic variants -V142I (0.241 AU, SD 0.008), -Val50Met (0.151 AU, SD 0.005) and -Phe53Leu (0.165 AU, SD 0.005) did show a significantly higher turbidity than wt-TTR (0.046 AU, SD 0.002) ($p < 0.0001$) (Fig. 2).

Additionally, the time course of protein aggregation was assessed over 24 h by turbidity assay. It showed that the attenuation of light scattering, hence protein aggregation, developed rather quickly, within the first 5 h, and reached almost saturation by the end of assessed time period. These data indicate that amyloid formation occurs rapidly in our assay and persists over time (Fig. 3).

Thioflavin T staining

ThT fluorescence of wt-TTR, pathogenic variants, and TTR-Ala65Val

This second assay was performed to survey whether detected protein aggregation was due to amyloid formation. ThT gains a new emission spectrum when it intercalates into amyloid fibrils. TTR-Ala65Val (57.54 AU, SD 10.13) as well as known pathogenic variants -Val142Ile

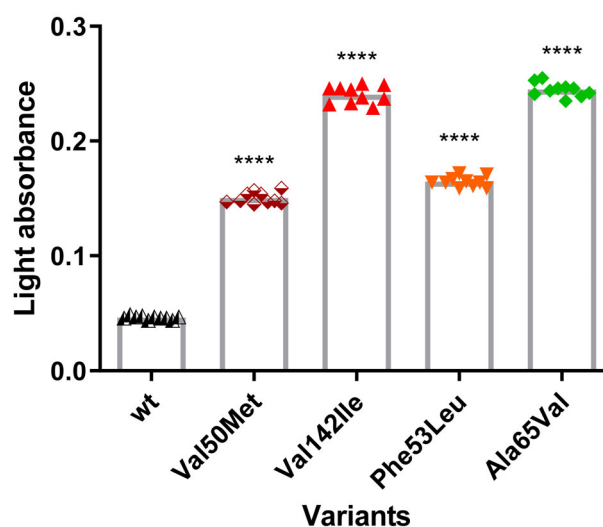


Figure 2. TTR-Ala65Val as well as positive controls TTR-Val50Met, -Val142Ile and -Phe53Leu show significantly higher light absorbance compared to wt-TTR in turbidity assay. Formation of amyloid fibrils increases solution's turbidity. Values show absorbance of light, which is a dimensionless unit. Measurements have been repeated twice and showed similar results. Blank values have been subtracted to erase background signal. One-way multiple comparison ANOVA-test was used for statistical analysis (**** $p < 0.0001$). TTR-variants were compared to wt-TTR.

(79.83 AU, SD 12.3), -Val50Met (54.71 AU, SD 13.07) and -Phe53Leu (55.57 AU, SD 9.73) did show a significantly higher emission signal compared to wt-TTR (17.63 AU, SD 3.59) ($p < 0.0001$) (Fig. 4).

ThT fluorescence of TTR-VUS

Pathogenic positive controls TTR-Val50Met (16.85 AU, SD 5.26) and -Val142Ile (33.54 AU, SD 10.13) showed a significant higher emission signal than wt-TTR, as expected (10.77 AU, SD 4.25) ($p > 0.0001$). TTR-Ala129Thr (9.27 AU, SD 4.14) was comparable to wt-TTR with no significant difference. The other tested variants, namely TTR-Gly26Ser (4.62 AU, SD 2.43), -Thr139Met (2.66 AU, SD 1.77), -Arg124Cys (3.77 AU, SD 2.42), -Pro122Arg (5.69 AU, SD 1.81), -Gly121Ser (4.88 AU, SD 3.26), -A129V (3.27 AU, SD 2.34), -Arg124His (6.77 AU, SD 6.46) showed a significantly lower emission signal compared to wt-TTR (Fig. 5). TTR-Gly26Ser has been used as a negative control, being a known benign variant. Furthermore, TTR-Thr139Met was also used as another negative control. It has been suggested to protect from ATTR amyloidosis.^{11,12}

Congo red and TTR-staining on patient samples

Congo red staining of P2 showed large amounts of amyloid deposits (Fig. 6). TTR co-staining confirmed that the

Figure 3. TTR-Ala65Val as well as positive controls TTR-Val50Met, -Val142Ile and -Phe53Leu show significantly higher turbidity after a few hours at acid conditions compared to wt-TTR in turbidity time course assay. Curves started to flatten soon and have almost flattened at the end of the assay. Values show absorbance of light, which is a dimensionless unit. Measurements have been repeated up to five times and showed similar results.

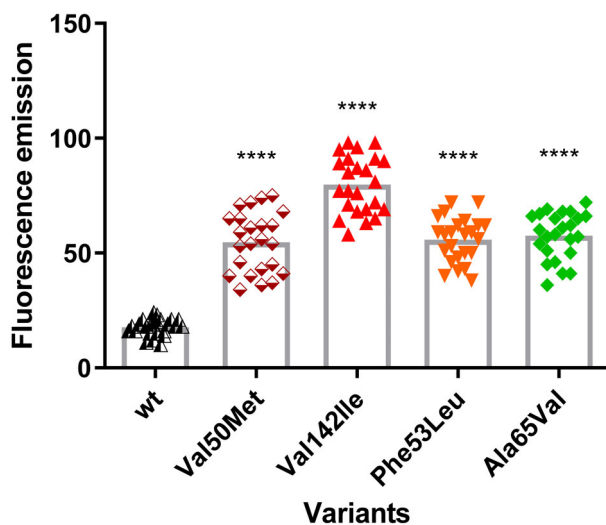
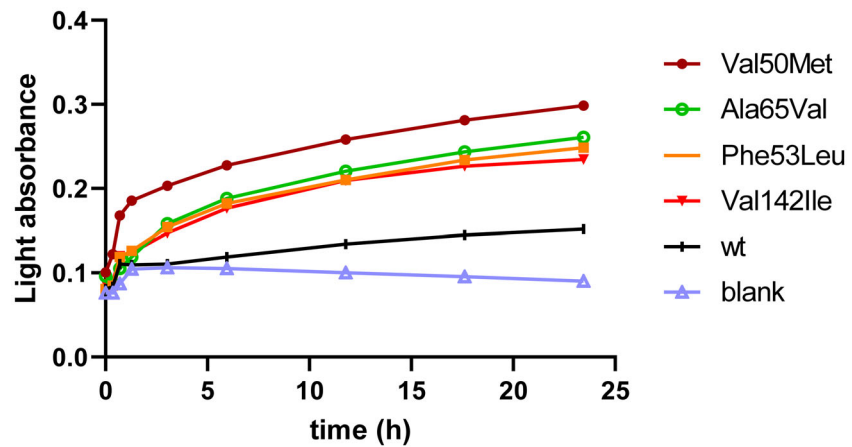


Figure 4. TTR-Ala65Val as well as positive controls TTR-Val50Met, -Val142Ile and -Phe53Leu show significantly higher light emission signal compared to wt-TTR in ThT-assay. ThT intercalates into amyloid fibrils. A new emission spectrum at 482 nm when excited at 450 nm shows the existence of amyloid fibrils. Values show fluorescence emission at 482 nm, which is an arbitrary unit. Measurements have been repeated twice and showed similar results. One-way multiple comparison ANOVA-test was used for statistical analysis (**** $p < 0.0001$). TTR-variants were compared to wt-TTR.

detected amyloid deposits were indeed TTR-deposits (Fig. 7). This result shows systemic ATTR-amyloidosis in P2. P1 had declined a tissue biopsy.

In silico analysis

All three known and the newly identified amino acid moiety causing aggregation are strictly involved in either hydrophobic or Van der Waals contacts (Fig. 8). TTR-Ala65Val, -Val50Met and -Val142Leu are hydrophobic core residues, which strictly stabilize the b-core of TTR (Fig. 8A). Only

TTR-Phe53Leu is oriented outwards, however, it plays a pivotal role in stabilizing the aggregated version (Fig. 8B). In contrast, amino acid moieties not causing aggregation can form electrostatic and or ionic interactions and are in their majority positioned to the exterior of the TTR β -structure (Fig. 8C). Interestingly, they appear in tandems in the amino acid sequence (TT, RR, AA) and mutations introduced cause a strict repulsive power destabilizing a potential aggregated form (Fig. 8D). For example, TTR-Thr139Met, -Arg124Cys/His, -Pro122Arg are structurally destabilizing the amyloid-like architecture.

Discussion

In this study, the utility of an experimental procedure consisting of cloning, expression, and measurement of protein aggregation and amyloid formation was performed to assess the overall amylogenic potential of TTR mutations. ThT as well as turbidity assay each were sufficiently sensitive to detect amyloid formation of known amylogenic TTR variants such as TTR-Val142Ile, -Val50Met, and -Phe53Leu. As expected, also wt-TTR showed some degree of amyloid aggregation, though emission remained significantly lower compared to the before mentioned pathogenic proteins.

TTR is a transport protein for vitamin A and thyroxine²³⁻²⁵ that is usually present as tetramer complex consisting of four TTR proteins. Spontaneous disintegration of those tetramers and misfolding of the monomers can result in ATTR_{wt} amyloidosis in people with normal genotypes, formerly called “senile systemic amyloidosis”.^{5,26,27,28} ATTR_{wt} amyloidosis usually occurs in high age, and often presents with cardiac symptoms.^{29,30} Pathogenic TTR-mutations drastically lower the stability of TTR tetramers or monomers and thereby increase the amyloidogenic properties of TTR, leading to ATTR_v amyloidosis, which is a rapid progressive, severe disease.

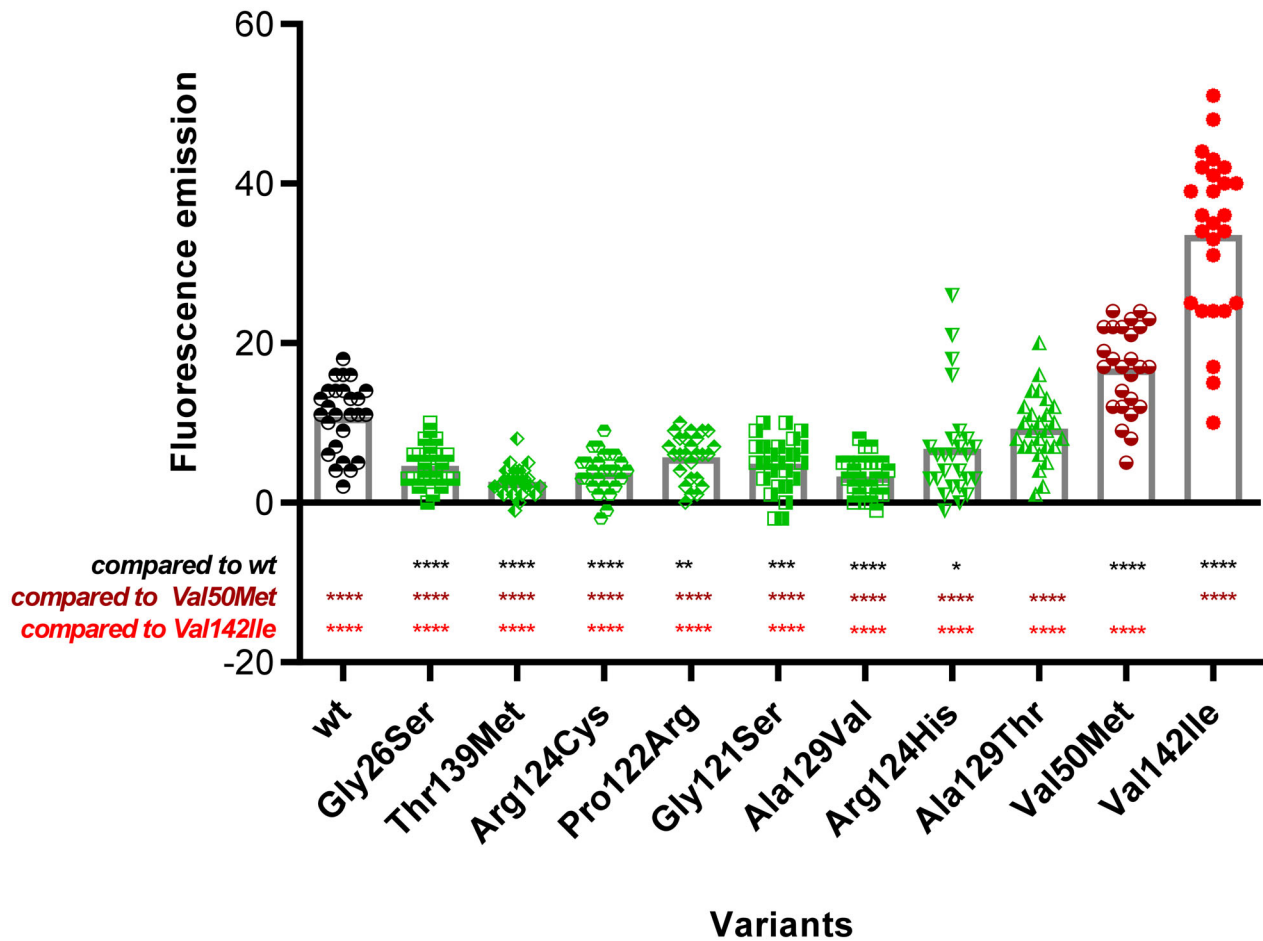


Figure 5. All tested TTR-VUS showed significantly lower fluorescence emission than of pathogenic positive controls TTR-Val50Met and TTR-Val142Ile. TTR-Ala129Thr showed comparable fluorescence emission than wt-TTR, all other VUS showed lower emission than wt-TTR in ThT-assay. Values show fluorescence emission at 482 nm when excited at 450 nm. Fluorescence emission is an arbitrary unit. Measurements have been repeated twice and showed similar results. One-way multiple comparison ANOVA-test was used for statistical analysis ($*p < 0.05$, $**p < 0.01$, $***p < 0.001$, $****p < 0.0001$). Significance levels of the top row refer to wt-TTR, the middle row refers to TTR-Val50Met, bottom row refers to TTR-Val142Ile.

Comparable to the tested known pathogenic variants, TTR-Ala65Val showed higher turbidity and higher light emission in ThT-assay, indicating a significantly higher amyloidogenic potential compared to wt-TTR. All other tested VUS had lower or similar emission compared to wt-TTR, and lower emission than tested pathogenic variants. Thus, we conclude that these are most likely not pathogenic and may even be protective by reducing protein aggregation.

Of the examined VUS, TTR-Gly26Ser is one of the rather frequent polymorphisms in caucasian population (4%–7%). We included TTR-Gly26Ser in our assays since there have been reports about symptomatic compound heterozygous (TTR-Gly26Ser/-Val50Met) carriers. Our data support the hypothesis that TTR-Gly26Ser was not responsible for the phenotype. Another tested variant was TTR-Thr139Met, which has been reported to be frequent

in the Portuguese population but does not go along with any signs of amyloid disease or family history of ATTRv amyloidosis, indicating to be an apathogenic variant.¹³ Moreover, it has been discussed in the past that TTR-Thr139Met could stabilize the TTR tetramer and thus be protective when being compound heterozygote (TTR-Val50Met/-Thr139Met).¹² Emission of TTR-Thr139Met was also significantly lower than wt-TTR in our Thioflavin T assay, which could point to a more stable TTR-form. Data of this work support the idea of TTR-Thr139Met being a protective variant. Likewise, TTR-Arg124His was also assessed, based on a report of a compound heterozygote carrier for TTR-Arg124His/-Val50Met. The index patient, 64 years old, had a slowly progressing peripheral neuropathy, gastrointestinal symptoms and disturbance of sight. Amyloid deposits were detected in the vitreous bodies. Other family members heterozygote for TTR-

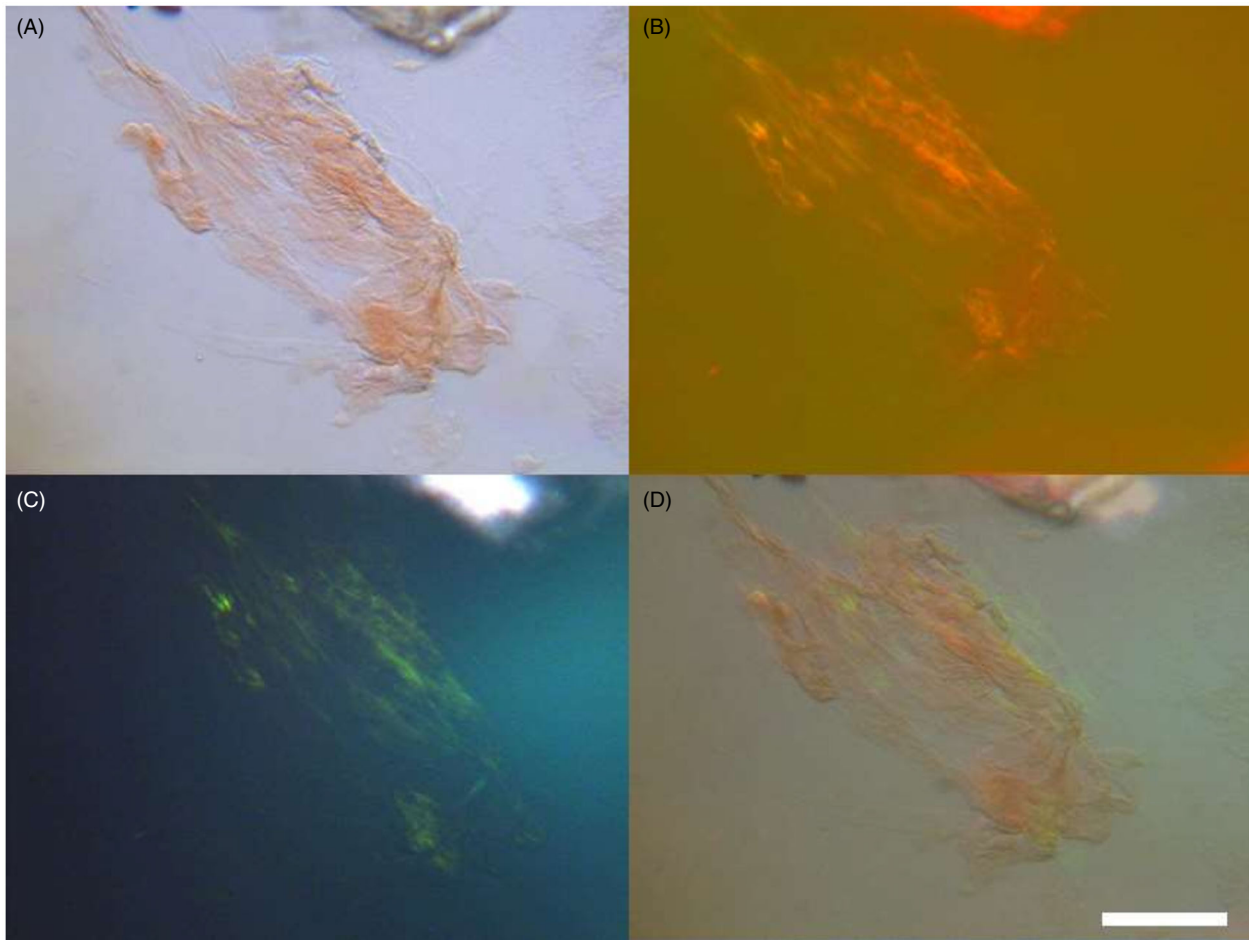


Figure 6. Diagnosis of the P2's amyloid. Native aspiration biopsy of fatty tissue pressed onto a glass slide and fixed with 10% of formalin, stained with Congo red and presented in microphotographs by triple illumination. (A) Congo red-stained tissue in bright-field microscopy, the amyloid appears red. (B) The same area as presented in A in fluorescence microscopy, amyloid shows a bright red signal. (C) The same section as in A shows the pathognomonic green birefringence under polarized light microscopy. (D) Is a merged image of (A) and (C). Scale bar represents 100 μm .

Arg124His including the 94-year-old father, the sister, and the two kids, showed no clinical phenotype. It indicates that TTR-Arg124His might play a suppressing role in the disease, since TTR-Arg124His/wt-TTR heterozygote family members were asymptomatic. Symptoms in the compound heterozygous patient developed only slowly compared to the usual rapid progression seen in ATTR_v amyloidosis. It has also been shown that tetrameric TTR-Arg124His/-Val50Met is more stable than TTR-Val50Met/wt-TTR.^{12,18} Data of this work supports this idea, showing significantly less amyloid formation than wt-TTR in vitro.

Another variant that we conclude to be apathogenic is TTR-Arg124Cys. It has been described in a 71-year old patient with sensory axonal peripheral neuropathy but no sign of amyloid deposits in muscle and nerve biopsies.¹⁴ Data show that TTR-Arg124Cys forms significantly fewer

amyloid fibrils than wt-TTR, suggesting that in this patient, the TTR-Arg124Cys variant was not the cause of the neuropathy.

The variant TTR-Pro122Arg, also not amylogenic in the described assays, has been reported in three members of a family without detectable signs of peripheral neuropathy.¹⁵ However, it was not described to which extent a clinical examination, nerve conduction studies or further examinations such as biopsies have been performed. TTR-Gly121Ser has been described in a 74-year old Japanese man, and this variant has been previously considered to be non-amylogenic. Recently, an experimental study suggested that TTR-G121S had an increased tetramer stability and thus was less likely to form amyloid than wt-TTR.¹⁶ This converges with the data of this study, that also show significantly less amyloid formation in vitro than wt-TTR. TTR-Ala129Val and -Ala129Thr were

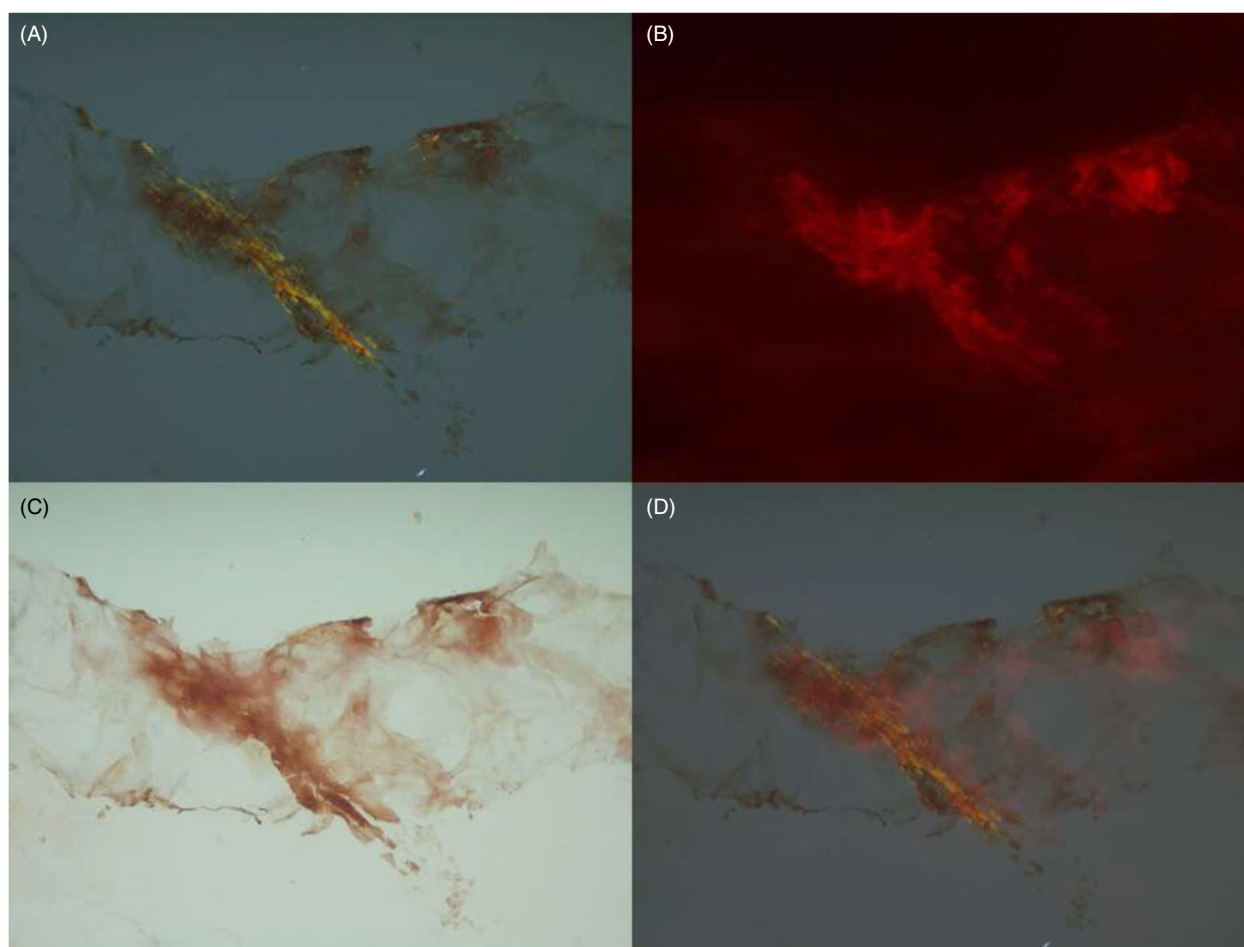


Figure 7. Diagnosis of the amyloid type as of TTR origin in double staining presented in triple illumination. (A) Green birefringence of amyloid under polarized light is pathognomonic for the presence of amyloid. (B) The same congo red stained section in fluorescence microscopy shows amyloid in brilliant red. (C) The amyloid appears in brown after immunohistochemical staining with Anti-TTR antibody. (D) Is a merged image of (A) and (C). Scale bar represents 100 μ m.

reported in single case reports and considered to be apathogenic but with insufficient clinical data provided to support this claim.^{13,17} Assays showed similar or lower amyloid levels than wild-type, suggesting that those mutations might not have an increased potential to form amyloid fibrils.

TTR-Ala65Val

To our knowledge, TTR-A65V has not been described in literature previously. We identified it in a family with at least two consecutive members, with P2 having a distinct polyneuropathy, and P1 showing initial symptoms and electrophysiological aberrations. Two different assays were performed to examine the amyloidogenic potential in vitro. Both assays showed an increased amyloidogenic potential. Time course analysis demonstrated a rapid fibril formation that was larger than that of wt-TTR over the

entire observation period. At the end of the assay, the curves had almost flattened completely, indicating that free TTR was consumed. It would be interesting to see amyloid formation in a more physiologic assay where TTR is constantly synthesized and added to the assay. Right now, the time course could simulate the fibril formation after a strict genetic knock down.

Additionally, congo red staining of fat tissue of P2 supported the idea of a systemic amyloidosis. TTR- and congo red co-staining supported the hypothesis that TTR-Ala65Val was responsible for the systemic amyloidosis and thus being a pathogenic variant leading to ATTR_v amyloidosis. It is important here to emphasize that even in case of an amyloid disease, one often fails to detect amyloid deposits in tissue biopsies. Hence, often biopsies alone are not sufficient to differentiate between benign and pathogenic variants. Thus, biochemical assays are useful especially in cases where one fails to detect amyloid deposits in biopsies.

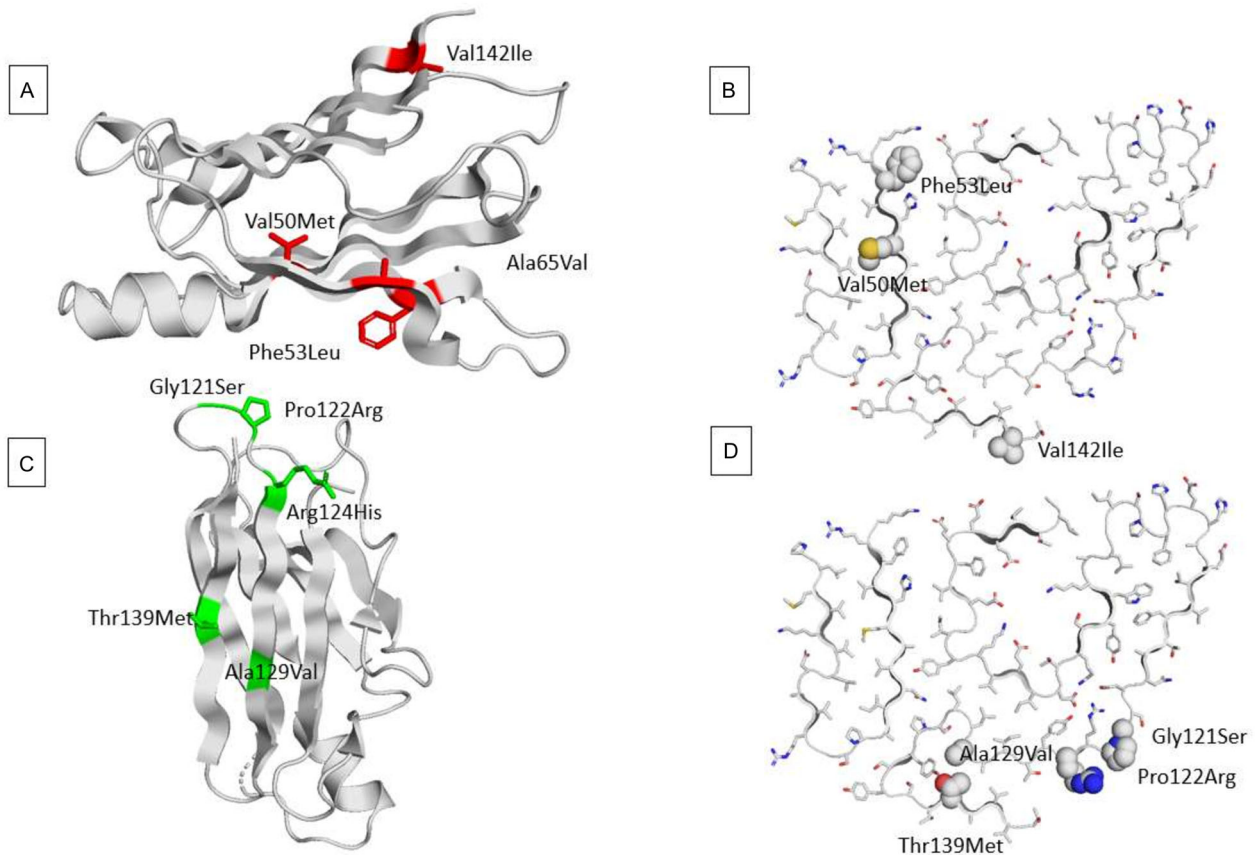


Figure 8. Comparison of amino acid positions aggregated (A and B) versus non-aggregated TTR (C and D). Left represents TTR according to pdb-code 4TLT. Right represents TTR according to pdb-code 6SDZ. The different mutations analyzed were marked.

Conclusion and prospect

This work suggests that TTR-Ala65Val is a pathogenic variant that was reported in one family with systemic ATTR amyloidosis and severe polyneuropathy. On the other hand, we could not detect an elevated amyloidogenic potential in TTR-Arg124Cys, -Pro122Arg, -Gly121Ser, -Ala129Val, -Arg124His and -Ala129Thr. Findings of this study show the value of *in vitro* assays to assess a variant's amyloidogenicity, even in cases where one fails to detect amyloid deposits in tissue biopsies. As described above, this is especially relevant because of low frequency and penetrance of ATTR_v amyloidosis, as well as high number of false-negative biopsies, which can be misleading. Since more VUS are to be found as genetic testing gets cheaper and ubiquitously available, we suggest *in vitro* assays to assess those variants' amyloidogenicity as well. A limitation of this approach is that we cannot definitely predict if and when a patient may develop clinical signs of amyloidosis. However *in vitro* assays may complement clinical data and could help in the decision making, if an anti-amyloidogenic therapy should be

initiated or not. *In silico* analysis showed differences in the variant's position, as well as in whether they are involved in either hydrophobic and van der Waals contacts, or in electrostatic and ionic interactions, depending on their pathogenicity. It might be a powerful tool to predict a variant's amyloidogenic properties, and as such might be helpful in the therapeutic decision making in the future.

Acknowledgments

We thank Jennifer Jost and Mahtab Taleb-Naghsh for excellent technical assistance. The study was funded by the German Research Foundation: FOR2722 to M. Koch. Open Access funding enabled and organized by Projekt DEAL. WOA Institution: Uniklinik Köln Consortia Name : Projekt DEAL

Author Contributions

(1) Conception and design of the study: HCL, MK, NBG, FN, TI, CS, MKRS. (2) acquisition and analysis of data:

NBG, FN, TI, RPL, JB, JSc, JSt. (3) drafting a significant portion of the manuscript or figures: HCL, MK, NBG, FN, TI, MD, CS, MKRS.

Conflict of Interest

This work was supported in part by a grant of Alnylam Pharmaceuticals. No drugs by this manufacturer were used in this study. No conflict to be reported.

References

1. Conceição I, González-Duarte A, Obici L, et al. 'Red-flag' symptom clusters in transthyretin familial amyloid polyneuropathy. *J Peripher Nerv Syst.* 2016;21:5-9.
2. Ando Y, Coelho T, Berk JL, et al. Guideline of transthyretin-related hereditary amyloidosis for clinicians. *Orphanet J Rare Dis.* 2013;8:31.
3. Jacobson DR, Pastore RD, Yaghoubian R, et al. Variant-sequence transthyretin (isoleucine 122) in late-onset cardiac amyloidosis in black Americans. *N Engl J Med.* 1997;336:466-473.
4. Sekijima Y. Transthyretin (ATTR) amyloidosis: clinical spectrum, molecular pathogenesis and disease-modifying treatments. *J Neurol Neurosurg Psychiatry.* 2015;86:1036-1043. doi:10.1136/jnnp-2014-308724
5. Colon W, Kelly JW. Partial denaturation of transthyretin is sufficient for amyloid fibril formation in vitro. *Biochemistry.* 1992;31:8654-8660.
6. Dohrn MF, Röcken C, Bleecker JL, et al. Diagnostic hallmarks and pitfalls in late-onset progressive transthyretin-related amyloid-neuropathy. *J Neurol.* 2013;260(12):3093-3108. doi:10.1007/s00415-013-7124-7
7. Dohrn MF, Medina J, Olaciregui Dague KR, Hund E. Are we creating a new phenotype? Physiological barriers and ethical considerations in the treatment of hereditary transthyretin-amyloidosis. *Neurol Res Pract.* 2021;3(1). doi:10.1186/s42466-021-00155-8
8. Hellman U, Alarcon F, Lundgren H-E, et al. Heterogeneity of penetrance in familial amyloid polyneuropathy, ATTR Val30Met, in the Swedish population. *Amyloid.* 2008;15:181-186.
9. Saporta MAC, Zaros C, Cruz MW, et al. Penetrance estimation of TTR familial amyloid polyneuropathy (type I) in Brazilian families. *Eur J Neurol.* 2009;16:337-341.
10. Yordanova I, Pavlova Z, Kirov A, et al. Monoallelic expression of the TTR gene as a contributor to the age at onset and penetrance of TTR-related amyloidosis. *Gene.* 2019;705:16-21.
11. Jacobson DR, Alves IL, Saraiva M, Thibodeau SN, Buxbaum JN. Transthyretin Ser 6 gene frequency in individuals without amyloidosis. *Hum Genet.* 1995;95(3):308-312. doi:10.1007/BF00225199
12. Almeida MR, Alves IL, Terazaki H, Ando Y, Saraiva MJ. Comparative studies of two transthyretin variants with protective effects on familial amyloidotic polyneuropathy: TTR R104H and TTR T119M. *Biochem Biophys Res Commun.* 2000;270:1024-1028.
13. Alves IL, Altland K, Almeida MR, Winter P, Saraiva MJ. Screening and biochemical characterization of transthyretin variants in the Portuguese population. *Hum Mutat.* 1997;9:226-233.
14. Saraiva MJM, Torres M, Serra J, Ochoa J. A new transthyretin variant-ATTR Arg 104 Cys. *Amyloid.* 1999;6:149-151.
15. do Rosário Almeda M, Altland K, Rauh S, et al. Characterization of a basic transthyretin variant - TTR Arg 102 - in the German population. *Biochim Biophys Acta.* 1991;1097:224-226.
16. Wakita Y, Sato T, Chosa K, et al. Characterization of non-amyloidogenic G101S transthyretin. *Biol Pharm Bull.* 2018;41:628-636.
17. Groenning M, Campos RI, Fagerberg C, et al. Thermodynamic stability and denaturation kinetics of a benign natural transthyretin mutant identified in a Danish kindred. *Amyloid.* 2011;18:35-46.
18. Terazaki H, Ando Y, Misumi S, et al. A novel compound heterozygote (FAP ATTR Arg104His/ATTR Val30Met) with high serum transthyretin (TTR) and retinol binding protein (RBP) levels. *Biochem Biophys Res Commun.* 1999;264:365-370.
19. Björkenheim A, Szabó B, Sztaniszláv AJ. Hereditary transthyretin amyloidosis caused by the rare Phe33Leu mutation. *BMJ Case Reports.* 2020;13(1):e232756. doi:10.1136/bcr-2019-232756
20. Groenning M. Binding mode of thioflavin T and other molecular probes in the context of amyloid fibrils—current status. *J Chem Biol.* 2010;3:1-18.
21. Linke RP. On typing amyloidosis using immunohistochemistry. Detailed illustrations, review and a note on mass spectrometry. *Prog Histochem Cytochem.* 2012;47:61-132.
22. Zhao R, So M, Maat H, et al. Measurement of amyloid formation by turbidity assay—seeing through the cloud. *Biophys Rev.* 2016;8:445-471.
23. Monaco H, Rizzi M, Coda A. Structure of a complex of two plasma proteins: transthyretin and retinol-binding protein. *Science.* 1995;268:1039-1041.
24. Schreiber G, Richardson SJ. The evolution of gene expression, structure and function of transthyretin. *Comp Biochem Physiol B Biochem Mol Biol.* 1997;116:137-160.
25. Wojtczak A, Cody V, Luft JR, Pangborn WA. Structures of human transthyretin complexed with thyroxine at 2.0 a resolution and 3',5'-dinitro-N-acetyl-L-thyronine at 2.2 a resolution. *Acta Crystallogr D Biol Crystallogr.* 1996;52:758-765.

26. Quintas A, Vaz DC, Cardoso I, Saraiva MJ, Brito RM. Tetramer dissociation and monomer partial unfolding precedes protofibril formation in amyloidogenic transthyretin variants. *J Biol Chem.* 2001;276:27207-27213.
27. Liepnieks JJ, Zhang LQ, Benson MD. Progression of transthyretin amyloid neuropathy after liver transplantation. *Neurology.* 2010;75:324-327.
28. Connors LH, Sam F, Skinner M, et al. Heart failure resulting from age-related cardiac amyloid disease associated with wild-type transthyretin: a prospective, observational cohort study. *Circulation.* 2016;133:282-290.
29. González-López E, Gallego-Delgado M, Guzzo-Merello G, et al. Wild-type transthyretin amyloidosis as a cause of heart failure with preserved ejection fraction. *Eur Heart J.* 2015;36:2585-2594.
30. Tanskanen M, Peuralinna T, Polvikoski T, et al. Senile systemic amyloidosis affects 25% of the very aged and associates with genetic variation in *alpha2-macroglobulin* and *tau*: a population-based autopsy study. *Ann Med.* 2008;40:232-239.